Simulation of Submicron Double-Heterojunction High Electron Mobility Transistors with MINIMOS-NT

Thomas Simlinger, Helmut Brech, Thomas Grave, and Siegfried Selberherr, *Fellow, IEEE*

***Abstract*— Simulations and measurements of submicron pseudomorphic high electron mobility transistors (HEMT's) are presented. For the simulations the generic device simulator MINIMOS-NT is used which is capable of dealing with complex device geometries as well as with several physical models represented by certain sets of partial differential equations. A description of the structure of the simulator is given, which shows the basic idea of splitting the device geometry into distinct regions. Within these "segments," arbitrary material properties and physical models, i.e., partial differential equations, can be defined independently. The segments are linked together by interface models which account for the interface conditions. The simulated characteristics of a HEMT with a gate length of 240 nm are compared with the measured data. Essential physical effects which determine the behavior of the device can be identified in the output and transfer characteristics.**

I. Introduction

In recent years, high electron mobility transistors (HEMT's) have become a widely used supplement to the spectrum of industrial semiconductor devices. Especially pseudomorphic submicron HEMT's have conquered a broad field of application because of their high-frequency performance.

The aim of this work is to show the capabilities and features of the two-dimensional (2-D) device simulator MINIMOS-NT which are required for the simulation of HEMT's. Special interface models are developed on the basis of DC-characteristics simulation of a pseudomorphic double-heterojunction AlGaAs/InGaAs HEMT with a gate length of 240 nm.

The simulation results are compared with measured data and three distinct operation regimes of the transfer characteristics can be diagnosed, each owing to a major physical effect. Identifying the essential physical mechanisms which are responsible for particular effects of the HEMT's electrical behavior by means of simulation allows to push ahead the further development of HEMT's. The capability of simulation includes device scaling as well as the potential of band gap engineering. Both improvements can be realized by process technology due to advances in epitaxial growth producing epilayers of almost arbitrary material composition.

Manuscript received April 27, 1996; revised November 12, 1996. The review of this paper was arranged by Editor B. Ricco.

T. Simlinger and S. Selberherr are with the Institute for Microelectronics, A-1040 Vienna, Austria.

H. Brech and T. Grave are with Corporate Research and Development, Siemens AG, D-81739 München, Germany.

Publisher Item Identifier S 0018-9383(97)02989-4.

The simulation of HEMT's is mainly facing two problems. Of concern are short-channel effects caused by reducing the gate length well below a quarter micron. Secondly, the device characteristics strongly depend on the properties of abrupt heterojunction interfaces.

To account for short-channel effects several attempts have been made to make the hydrodynamic (HD) model suitable for device simulation [1]–[4]. However, the convergence of the HD model is poor and the computational effort is high, since the set of unknowns is augmented by the carrier energies. Both effects can be mitigated when the HD model is only used for regions of the device where nonlocal behavior is dominating, hence by mixing drift-diffusion (DD) and hydrodynamic model (mixed-model simulation). For HEMT's the critical region is the channel layer. To apply the HD model only for the channel layer, this region must be cut out and then linked with the remaining regions by specific interface models. Thus, the device region is split into a set of subdomains by a process referred to as segment split method (SSM) [5].

Moreover, the SSM offers an elegant way to handle abrupt heterojunctions using specific interface models mentioned above. Previously published simulators are only capable of dealing with continuous material properties [6], [7] and therefore ignoring thermionic-field emission, or they are designed for only one dimension in space [8], [9]. Using SSM it is possible to combine models for abrupt heterojunctions and 2-D device simulation. Accordingly, for the simulation of HEMT's the short-channel effects can be considered as well as the influence of the thermionic-field emission on the confinement of the electrons inside the channel layer.

In Section II the equations for the drift-diffusion and hydrodynamic models, the interface model for thermionic-field emission, and the physical models are presented along with some notes on numerics. The measured DC characteristics are compared with simulation results in Section III as well as a discussion of several physical effects which influence the transfer characteristics. Finally, some conclusions are presented in Section IV.

II. Segment Split Method and Mixed Drift-Diffusion Hydrodynamic Simulation

The electrical behavior of the HEMT is mainly determined by the epitaxial grown structure of the device. Several distinct layers of different semiconductor alloys are combined to obtain a channel with high electron mobility and high electron concentration. The properties of the channel are expected to govern the electron transport (see Fig. 1). The

0018–9383/97$10.00 © 1997 IEEE

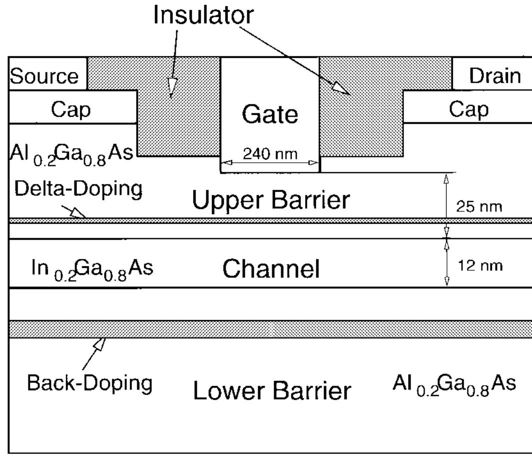

Fig. 1. Schematic cross section of a delta-doped pseudomorphic double-heterojunction HEMT. The current is conducted inside the narrow band-gap $In_{0.2}Ga_{0.8}As$ channel layer, 12 nm thick, which is sandwiched between the wide band-gap $Al_{0.2}Ga_{0.8}As$ upper and lower barrier layer.

material and electrical properties change almost abruptly at the heterojunction interfaces, i.e., at interfaces between different layers. Inside a layer the material properties and the electrical quantities are continuous, and the partial differential equations (PDE) describing the electrical behavior can be solved numerically. The discontinuous behavior on interfaces between layers has to be treated by specific interface models to link the layers together. For the simulation the device domain is split into several subdomains, referred to as segments. Each segment corresponds to a distinct layer of the device. This process is termed segment split method (SSM).

Abrupt heterojunction interfaces can be properly handled with interface models. Especially, the effects of tunneling through energy barriers at heterojunction interfaces can be considered analytically for arbitrary device geometries. Tunneling is important to describe the electron transport from the drain-sided end of the channel into the barrier layer above. Furthermore, by linking segments with different properties by appropriate interface models, the models for the segments can also be different. Thus, for the channel segment a five equation hydrodynamic (HD) model can be used to account for short-channel effects and a plain three equation drift-diffusion (DD) model for the other segments. Compared to simulations using the HD model for the entire device, mixed DD/HD model simulations are more effective with respect to computation time and the convergence of the iteration scheme.

A. Basic Equations

In the following the basic equations used for the simulation of the HEMT are given. For plain drift-diffusion modeling the well known Poisson equation and continuity equations are used. Additionally, to account for short-channel effects, a hydrodynamic model describing the energy transport is implemented and the continuity equations are extended for nonconstant carrier temperatures.

The Poisson and continuity equations read

$$\nabla(\varepsilon \cdot \nabla\psi) - q \cdot (n - p + N_A^- - N_D^+ - N_{DD}^+) = 0 \quad (1)$$

$$\nabla \vec{J}_n - q \cdot \frac{\partial n}{\partial t} - q \cdot R = 0 \quad (2)$$

$$\nabla \vec{J}_p + q \cdot \frac{\partial p}{\partial t} + q \cdot R = 0 \quad (3)$$

where $\vec{J}_n$ and $\vec{J}_p$ are the electron and hole current densities, respectively, R is the net recombination rate, ε is the permittivity, n and p the electron and hole concentrations, q is the absolute electron charge, N_A^- and N_D^+ are the densities of ionized acceptors and donors, and N_{DD}^+ is the density of ionized deep traps, respectively.

The current densities are defined as

$$\vec{J}_n = q \cdot \mu_n \cdot n \cdot \left[\nabla\left(\frac{E_C}{q} - \psi\right) + \frac{k}{q} \cdot \frac{N_C}{n} \cdot \nabla \frac{n \cdot T_n}{N_C}\right] \quad (4)$$

$$\vec{J}_p = q \cdot \mu_p \cdot p \cdot \left[\nabla\left(\frac{E_V}{q} - \psi\right) - \frac{k}{q} \cdot \frac{N_V}{p} \cdot \nabla \frac{p \cdot T_p}{N_V}\right] \quad (5)$$

where the nonconstant carrier temperatures and effective-density-of-states are considered by the terms $\nabla(n \cdot T_n/N_C)$ and $\nabla(p \cdot T_p/N_V)$, respectively. The terms $\nabla(E_C/q - \psi)$ and $\nabla(E_V/q - \psi)$ account for the nonconstant band edge energies. The definition of the carrier mobilities μ_n and μ_p depends on the applied model and considers a field dependence for the DD model and a carrier temperature dependence for the HD model.

For the HD model the equations governing the energy transport are

$$\nabla \vec{S}_n + \frac{\partial(n \cdot w_n)}{\partial t} - \nabla\left(\frac{E_C}{q} - \psi\right) \cdot \vec{J}_n + n \cdot \frac{w_n - w_0}{\tau_{wn}} + w \cdot R = 0 \quad (6)$$

$$\nabla \vec{S}_p + \frac{\partial(p \cdot w_p)}{\partial t} - \nabla\left(\frac{E_V}{q} - \psi\right) \cdot \vec{J}_p + p \cdot \frac{w_p - w_0}{\tau_{wp}} + w \cdot R = 0 \quad (7)$$

where

$$\vec{S}_n = -\kappa_n \cdot \nabla T_n - \frac{1}{q} \cdot (w_n + k \cdot T_n) \cdot \vec{J}_n \quad (8)$$

$$\vec{S}_p = -\kappa_p \cdot \nabla T_p + \frac{1}{q} \cdot (w_p + k \cdot T_p) \cdot \vec{J}_p \quad (9)$$

are the electron and hole energy fluxes, respectively, τ_{wn} and τ_{wp} are the energy relaxation times, and w_n and w_p are the electron and hole energies, respectively. Since the simulations are performed for room temperature $T = 300$ K the drift kinetic energy part is small compared to the random kinetic energy of the carriers and can be neglected

$$w_{np} \approx \tfrac{3}{2} \cdot k \cdot T_{np}. \quad (10)$$

For the thermal conductivities the Wiedemann–Frantz–Law is used

$$\kappa_{np} = \frac{5}{2} \cdot \frac{k^2}{q} \cdot T_{np} \cdot \mu_{np} \cdot (n, p). \quad (11)$$

Furthermore, for the discretization of the continuity and energy balance equations we implemented the scheme proposed in [3] to improve the poor convergence behavior of the HD model.

B. Interface Models

Considering the interface between Segment 1 and Segment 2, the thermionic-field emission model determines the electron current density J_{n1} leaving Segment 1, the electron current density J_{n2} entering Segment 2, the electron energy flux density S_{n1} leaving Segment 1, and the electron energy flux density S_{n2} entering Segment 2

$$J_{n2} = J_{n1} \tag{12}$$

$$S_{n2} = S_{n1} + \frac{1}{q} \cdot (\Delta E_C - \delta E_C) \cdot J_{n2} \tag{13}$$

$$J_{n2} = q \cdot v_{n2}(T_{n2}) \cdot n_2 - q \cdot \frac{m_{n2}}{m_{n1}} \cdot v_{n1}(T_{n1}) \cdot n_1 \cdot \exp\left(-\frac{\Delta E_C - \delta E_C}{k \cdot T_{n1}}\right) \tag{14}$$

$$S_{n2} = -2 \cdot k \cdot T_{n2} \cdot v_{n2}(T_{n2}) \cdot n_2 + 2 \cdot \frac{m_{n2}}{m_{n1}} \cdot k \cdot T_{n1} \cdot v_{n1}(T_{n1}) \cdot n_1 \cdot \exp\left(-\frac{\Delta E_C - \delta E_C}{k \cdot T_{n1}}\right) \tag{15}$$

where

$$v_{n1,2}(T_{n1,2}) = \sqrt{\frac{2 \cdot k \cdot T_{n1,2}}{\pi \cdot m^*_{n1,2}}} \tag{16}$$

denotes the "emission velocity," and $m^*_{n1,2}$ are the electron effective masses for Segments 1 and 2, respectively. The barrier height is defined as

$$\Delta E_C = E_{C2} - E_{C1}. \tag{17}$$

For the electrostatic potential the interface condition reads

$$\psi_1 = \psi_2. \tag{18}$$

Tunneling of electrons through the energy barrier is taken into account by barrier height lowering, which is modeled as

$$\delta E_C = \begin{cases} q \cdot E_\perp \cdot x_{\text{eff}} & E_\perp > 0 \\ 0 & E_\perp \leq 0 \end{cases} \tag{19}$$

where $E_\perp$ is the electric field perpendicular to the interface in Segment 2 and x_{eff} is the effective tunnel length which is assumed with 7 nm.

The exponential term in (14) containing the barrier height determines the current flow across the interface. The effectiveness of this energy barrier is reduced either by barrier height lowering due to tunneling or by increasing electron temperature T_{n1}. Thus, the carrier temperature influences the current flux across the interface—the higher the electron temperature the more electrons are able to surmount the energy barrier. This effect is referred to as real-space transfer (RST, [10]).

The mixed DD/HD model simulation requires a suitable value for the electron temperature T_{n2} inside the wide band-gap semiconductor segment where the carrier temperature is not calculated explicitly. One possibility is to assume the carrier temperature identical to the lattice temperature. However, full HD simulations show that the carrier temperature does not change very much in the vicinity of the interface. Thus, for mixed-model simulation the carrier temperatures on both sides of the interface are supposed to be equal $(T_{n1} = T_{n2})$.

C. Numerical Methods

The discretized nonlinear equation system is solved by a Newton–Raphson scheme. Additionally, to improve the well known poor convergence of the energy transport equations a block iterative scheme is implemented. First, the set of Poisson equation and continuity equations is solved alternately with the set of continuity equations and energy transport equations. Each set is solved iteratively by the Newton–Raphson method until the norm of the updates remains under a certain value. At last, for the full equation set the Newton–Raphson method [11], [12] is invoked to obtain the desired final accuracy. The linear system is solved either by a Gauß-solver or by a state-of-the-art BiCGStab algorithm [13]. When the BiCGStab algorithm is employed, at first the matrix is scaled with an iterative algorithm [14] and preconditioned [15].

D. Physical Models

In the sequel the models for the band edge energies [16], the electron and hole effective masses [16], and the mobilities for $Al_xGa_{1-x}As$ and $In_yGa_{1-y}As$ are given.

Usually, the band gap energies are used for simulation. However, the correct treatment of the abrupt heterojunctions requires the energy barrier height on the interfaces, i.e., the values for the conduction band edge energy and the valence band edge energy as well.

The band gap energy for $Al_xGa_{1-x}As$ reads

$$E_g(x,T) = E_g(x,0) - \frac{\alpha(x) \cdot T^2}{\beta(x) + T} \tag{20}$$

$$E_g(x,0) = E_g^{\text{GaAs}} \cdot (1-x) + E_g^{\text{AlAs}} \cdot x \tag{21}$$

$$\alpha(x) = \alpha^{\text{GaAs}} \cdot (1-x) + \alpha^{\text{AlAs}} \cdot x \tag{22}$$

$$\beta(x) = \beta^{\text{GaAs}} \cdot (1-x) + \beta^{\text{AlAs}} \cdot x \tag{23}$$

where $E_g(x,T)$ is given in eV and T is the lattice temperature in K.

The band gap energy for InAs reads

$$E_g^{\text{InAs}}(T) = E_g^{\text{InAs}} - \frac{\alpha^{\text{InAs}} \cdot T^2}{\beta^{\text{InAs}} + T} \tag{24}$$

with the appropriate parameters $E_g^{\text{InAs}}, \alpha^{\text{InAs}}$, and β^{InAs} (see Table I).

The band gap energy for $In_yGa_{1-y}As$ is given by

$$E_g(y,T) = E_g^{\text{GaAs}}(T) \cdot (1-y) + E_g^{\text{InAs}}(T) \cdot y - C \cdot y^2 \tag{25}$$

where $E_g^{\text{GaAs}}(T)$ and $E_g^{\text{InAs}}(T)$ are the band gap energies for GaAs and InAs, respectively, and C is the "bowing" parameter [16]. For the values of the parameters, see Table I.

The band gap energy is related to the band edge energies by

$$E_C(x,T) = E_g(0,T) + 0.6 \cdot [E_g(x,T) - E_g(0,T)] \tag{26}$$

$$E_V(x,T) = E_C(x,T) - E_g(x,T) \tag{27}$$

thus, 60% of the change of the band gap energy are attributed to the conduction band edge energy and 40% to the valence band edge energy.

TABLE I
PARAMETER VALUES FOR MODELING THE BAND GAP ENERGIES

α^{GaAs} [10^{-4}eV/K]	α^{AlAs} [10^{-4}eV/K]	α^{InAs} [10^{-4}eV/K]
5.58	8.78	2.76
β^{GaAs} [K]	β^{AlAs} [K]	β^{InAs} [K]
220	322	83
E_g^{GaAs} [eV]	E_g^{AlAs} [eV]	E_g^{InAs} [eV]
1.521	2.891	0.42
C [eV]	0.475	

TABLE II
PARAMETER VALUES FOR MODELING THE CARRIER EFFECTIVE MASSES

Parameter	AlGaAs	InGaAs
$m0_{\mathrm{n}}$	+0.067	+0.079
$m1_{\mathrm{n}}$	+0.083	−0.038
$m2_{\mathrm{n}}$		
$m0_{\mathrm{p}}$	+0.080	+0.120
$m1_{\mathrm{p}}$	+0.080	−0.099
$m2_{\mathrm{p}}$	–	+0.030

TABLE III
PARAMETER VALUES FOR THE MOBILITY MODELS

Parameter	AlGaAs	InGaAs
μ_{n}^0 [cm^2/Vs]	3000	6000
$v_{\mathrm{n}}^{\mathrm{sat}}$ [cm/s]	$8.0 \cdot 10^6$	$11.0 \cdot 10^6$
α_{n} [K^{-1}]	0.0431	0.0064
μ_{p}^0 [cm^2/Vs]	120	120
$v_{\mathrm{p}}^{\mathrm{sat}}$ [cm/s]	$5.0 \cdot 10^6$	$5.0 \cdot 10^6$
α_{p} [K^{-1}]	$0.62 \cdot 10^{-3}$	$0.62 \cdot 10^{-3}$

The carrier effective masses for $Al_xGa_{1-x}As$ read

$$m_{np}^* = m0_{np} + m1_{np} \cdot x + m2_{np} \cdot x^2 \tag{28}$$

where for $x = 0$ the effective masses for GaAs are obtained. Table II shows the values used for these parameters.

The carrier effective masses for $In_yGa_{1-y}As$ are governed by

$$m_{np}^* = m0_{np} + m1_{np} \cdot y + m2_{np} \cdot y^2 \tag{29}$$

where the effective masses for InAs are obtained with $y = 1.0$ (see Table II).

The DD mobility is modeled by

$$\mu_{np}(|\vec{F}_{np}|) = \frac{\mu_{np}^0}{\sqrt{1 + \left(\frac{\mu_{np}^0 \cdot |\vec{F}_{np}|}{v_{np}^{\mathrm{sat}}}\right)^2}} \tag{30}$$

where μ_{np}^0 are the zero-field mobilities, v_{np}^{sat} are the saturation velocities, and $|\vec{F}_{np}|$ are the magnitudes of the driving force for electrons and holes, respectively. The driving forces are governed by the equations

$$\vec{J}_n = q \cdot n \cdot \mu_n \cdot \vec{F}_n, \quad \vec{J}_p = q \cdot p \cdot \mu_p \cdot \vec{F}_p. \tag{31}$$

The HD mobility is modeled carrier temperature dependent

$$\mu_{np}(T_{np}) = \frac{\mu_{np}^0}{1 + \alpha_{np}(T_{np} - T_L)} \tag{32}$$

where T_{np} are the carrier temperatures and T_L is the lattice temperature. The corresponding values for the parameters can be found in Table III.

III. RESULTS

The device simulated in this study was fabricated using a structure grown by molecular beam epitaxy. From top to bottom the layer sequence consists of a highly doped GaAs cap layer, a 30 nm undoped $Al_{0.2}Ga_{0.8}As$ upper barrier layer, a 12 nm $In_{0.2}Ga_{0.8}As$ channel layer, and a 400 nm $Al_{0.2}Ga_{0.8}As$ lower barrier layer on a semi-insulating GaAs-substrate. Within the upper barrier layer, a delta doping with an active doping concentration of about $N_D = 2.7 \cdot 10^{12}$ cm^{-2} is grown. The $Al_{0.2}Ga_{0.8}As$ barrier below the channel contains a 7 nm thick doping layer with an active doping concentration of about $N_D = 8.5 \cdot 10^{11}$ cm^{-2}.

The gate length of the HEMT is 240 nm. In the vicinity of the gate, the cap layer is etched to form a recess of about 540 nm length. The gate is placed symmetrically within the recess. Thus, ungated channel regions extend for about 150 nm at both sides of the gate. Fig. 2 shows a representative SEM-profile (Scanning Electron Microscopy) of the structure. As can be seen, the alloying process of the ohmic contacts does not lead to complete penetration of the cap. Thus, we assume that the underlying heterostructures are not destroyed by the contacts. Therefore, the schematic structure shown in Fig. 1 where the ohmic metal is placed on top of the cap layer is used for simulation. For the 2-D simulations a contact resistance of 0.1 Ω·mm is assumed. The width of the device is 180 μm which results in a contact resistance of 0.6 Ω for the complete extrinsic device.

The mixed-model simulation is performed with a hydrodynamic model within the channel region and a drift-diffusion model within the other layers. The hydrodynamic model is only applied to electrons. The hole concentration does not influence the device characteristics and their temperature is held constant at 300 K. A rectangular grid with 2726 points is used for discretization. The channel layer is discretized with 315 points. Thus, the mixed DD/HD model simulation needs about 1.2 times the computation time of a plain DD simulation and at least 0.7 times the computation time of a full HD simulation.

The simulation of one bias point requires an average of 500 iteration steps, 30 MB main memory, and needs 200 s. CPU-time on an HP 9000/735 with 100 MHz clock frequency.

The measured transfer characteristic for a drain-source voltage of 2 V is shown in Fig. 3 along with three simulated I–V curves, one with plain DD model simulation, one with mixed-model simulation, and one with full HD model simulation. The measurement was performed on wafer on a 4×45 μm device. As depicted in this figure the mixed-model simulation and the measured data agree very well. Furthermore, the full HD

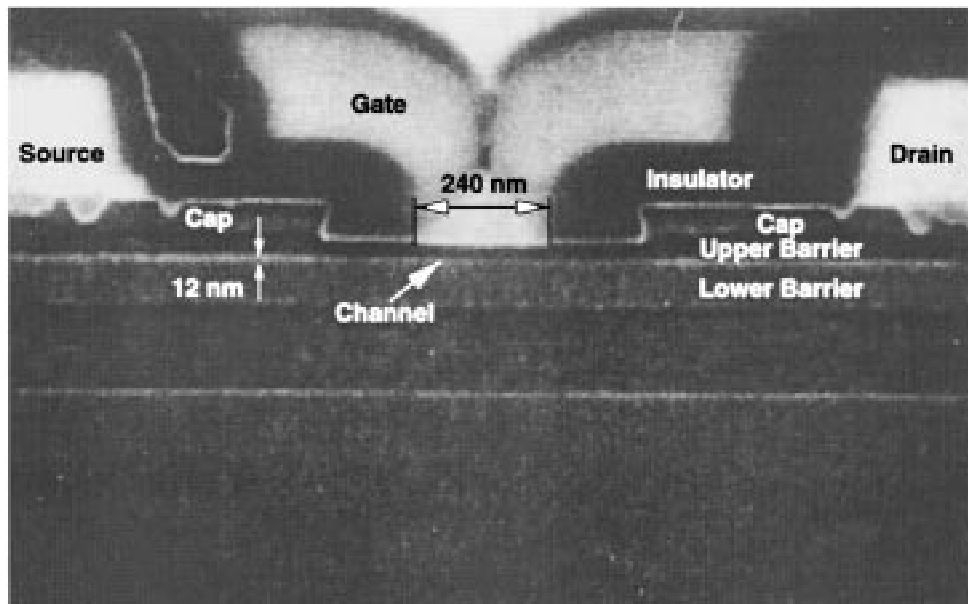

Fig. 2. Representative scanning electron microscopy cross section of the HEMT.

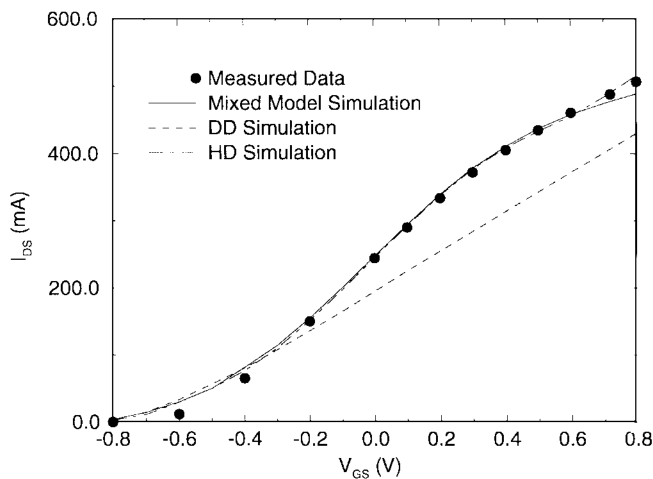

Fig. 3. I–V curves for $V_{DS} = 2$ V.

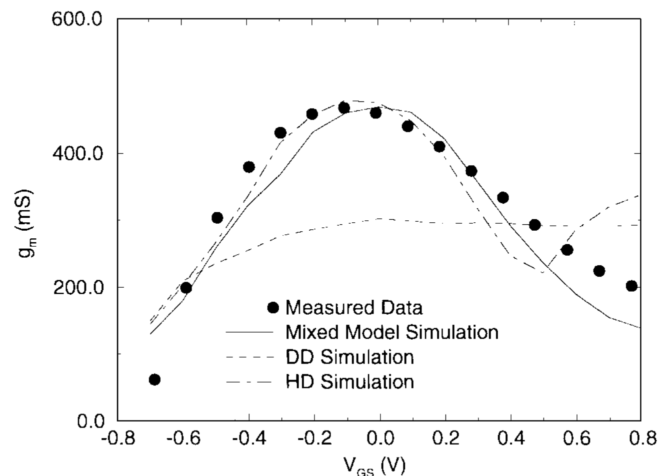

Fig. 4. Transconductance for $V_{DS} = 2$ V.

model and mixed-model simulations are almost identical. For gate voltages higher than 0.6 V the full HD model simulation shows an increase of the drain current which can be attributed to a parasitic channel in the upper barrier layer. This parasitic channel is also shown by mixed-model simulations but for gate voltages beyond 0.8 V. A detailed investigation of the parasitic-channel effect will be published in another paper.

The transfer characteristics can be divided up into three operation regimes, each regime owing to a major physical effect. Firstly, the pinch off regime, i.e., negative gate voltages where the electron concentration in the channel is low but is starting to rise with the gate voltage increasing. Most of the current flowing is conducted in the lower barrier layer.

The deviation of the DD simulation and the measurement can be attributed to an overestimation of the electron confinement in the channel, i.e., the electrons are not swapped out into the lower barrier where their mobility is rather low. This is simulated much more realistically by the mixed-model simulation as shown in Fig. 6.

The second regime is the one of most interest for device applications. The drain current is controlled mostly linear by the gate voltage and exhibits the maximum in g_m, as shown in Fig. 4.

For gate voltages higher than 0.3 V, marking the third regime, the I–V curve in Fig. 3 drops off since the electrons heat up and start to surmount the energy barrier between channel and the barrier layer above known as real-space transfer of the electrons. Hence, an increasing fraction of the electron transport takes place within the upper barrier layer where the electron mobility is much lower than within the channel. Fig. 5 shows the electron temperature inside the channel of the transistor and Fig. 7 the electron concentration of the entire device. As clearly can be seen in Fig. 5 the temperature is about 3000 K on the drain-sided end of the channel which allows the electrons easily to cross the heterojunction between channel and upper barrier layer.

Tunneling of electrons through the heterojunctions is important for the connection of the drain-sided end of the channel

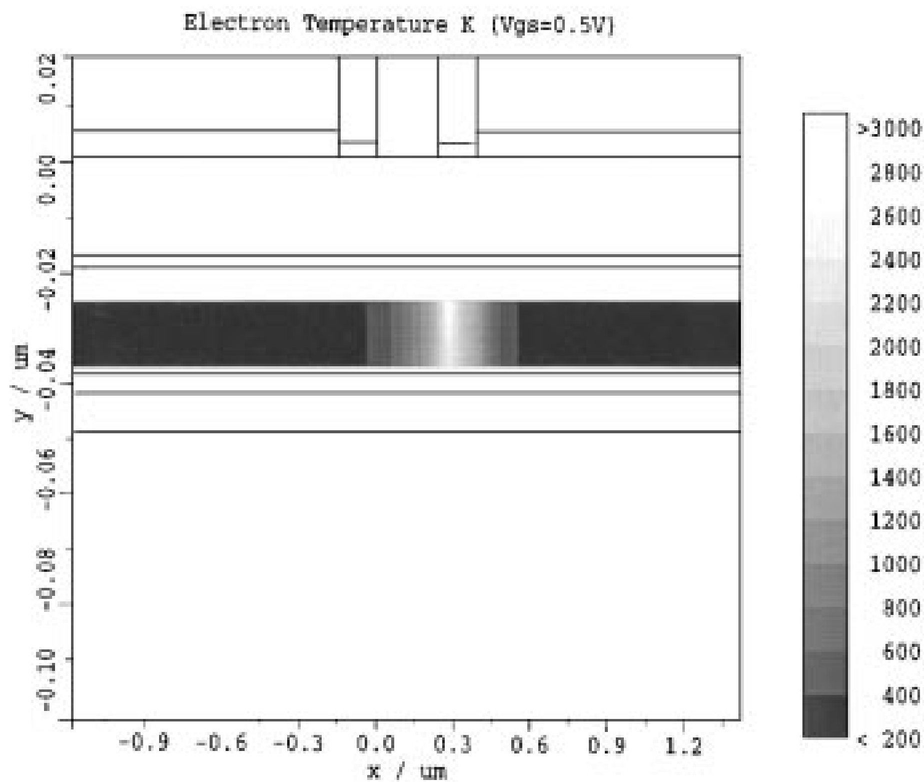

Fig. 5. Electron temperature inside the channel layer ($V_{DS} = 2$ V, $V_{GS} = +0.5$ V).

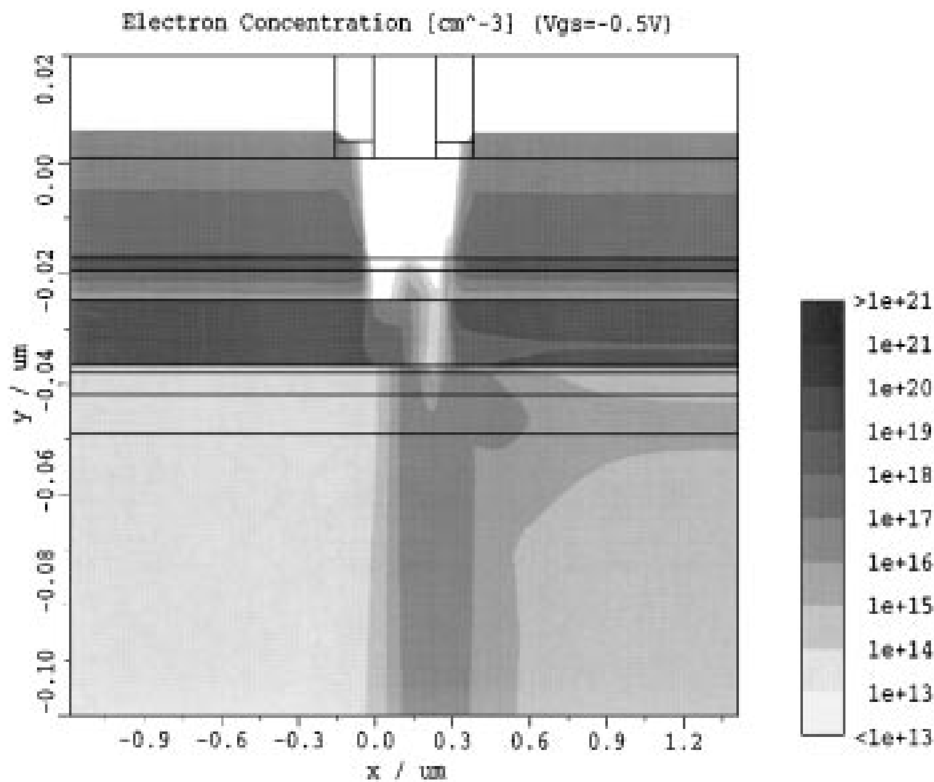

Fig. 6. Electron concentration ($V_{DS} = 2$ V, $V_{GS} = -0.5$ V).

to the drain contact. When tunneling is not taken into account only few electrons are able to leave the channel and to reach the drain contact. Thus, the current is correspondingly too low (see Fig. 3).

In Fig. 8 the output characteristics of the HEMT are depicted. The simulation results are in good agreement with the measured data. The correspondence of the output conductance shows, that, as stated above, the current flow inside the channel

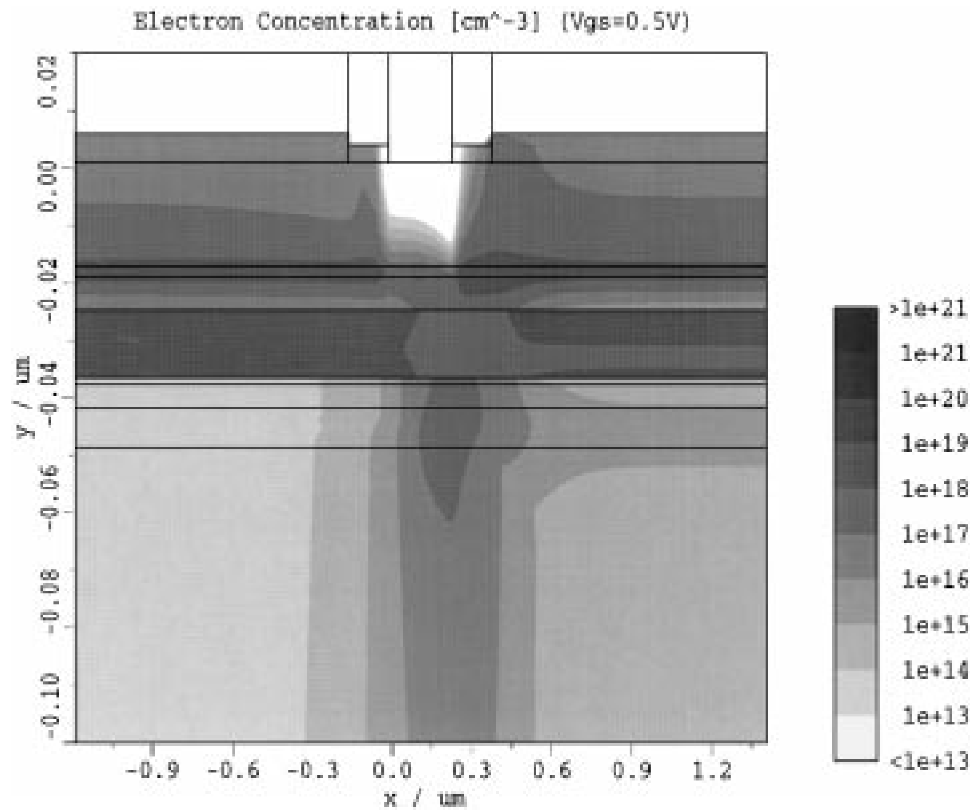

Fig. 7. Electron concentration ($V_{DS} = 2$ V, $V_{GS} = +0.5$ V).

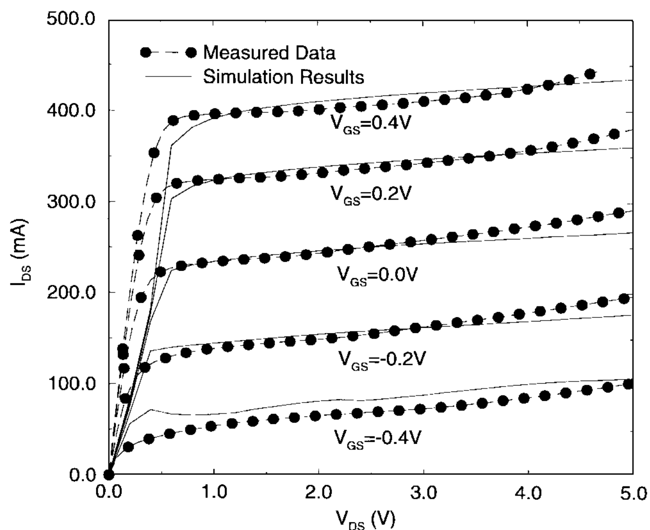

Fig. 8. Output characteristics of the HEMT. The simulation results are in good agreement with the measured data except for drain-source voltages below 0.5 V. The inaccuracy of the results for the ohmic operation regime is induced by the exponential dependence of the tunneling model on the electrical field at the heterojunction interface.

and the neighboring segments is well characterized by the mixed-model simulations. The disagreement of the simulations and the measurements for drain-source voltages below 0.5 V is due to the tunneling model. The tunneling current across the heterojunction depends exponentially on the perpendicular component of the electric field at the interface, the calculation of which is very inexact. This exponential dependence causes the inaccuracy of the model for the ohmic operation regime of the HEMT. Further improvement of the tunneling model will alleviate this problem.

IV. Conclusion

A quarter micron delta-doped pseudomorphic double-heterojunction high electron mobility transistor is simulated with the generic 2-D device simulator MINIMOS-NT. A new method is used which divides the device region into several subdomains, referred to as segments, each segment with its specific physical models. This offers the opportunity to combine segments where a hydrodynamic model is used with segments where the plain drift-diffusion model is employed. Thus, for the channel of the transistor, where short-channel effects are expected, the energy balance equations are used to account for nonlocal effects such as velocity overshoot. Furthermore, solving the hydrodynamic model in only a part of the device is more efficient than a full hydrodynamic solution.

Moreover, the distinct segments are linked together with specific interface models. These interface models allow to deal with abrupt heterojunctions and to include the effects of thermionic-field emission which determine the current confinement within the channel layer and properly describe how the carriers swap out into the neighboring segments. Hence, the reduction of the transconductance by real-space transfer can be observed by the simulations.

The combination of abrupt heterojunctions and a 2-D mixed hydrodynamic drift-diffusion model simulation leads to reasonable results which are in good agreement with the measured data. Furthermore, the influence of several physical effects, such as real-space transfer and carrier heating, on the device characteristics can be identified.

REFERENCES

[1] A. Forghieri, R. Guerrieri, P. Ciampolini, A. Gnudi, M. Rudan, and G. Baccarani, "A new discretization strategy of the semiconductor equations comprising momentum and energy balance," *IEEE Trans. Computer-Aided Design*, vol. 7, pp. 231–242, Feb. 1988.

[2] T. Tang, "Extension of the Scharfetter-Gummel algorithm to the energy balance equation," *IEEE Trans. Electron Devices*, vol. ED-31, pp. 1912–1914, Dec. 1984.

[3] W.-S. Choi, J.-G. Ahn, Y.-J. Park, H.-S. Min, and C.-G. Hwang, "A time dependent hydrodynamic device simulator SNU-2D with new discretization scheme and algorithm," *IEEE Trans. Computer-Aided Design*, vol. 13, pp. 899–908, Jul. 1994.

[4] T.-W. Tang and M.-K. Ieong, "Discretization of flux densities in device simulations using optimum artificial diffusivity," *IEEE Trans. Computer-Aided Design*, vol. 14, pp. 1309–1315, Nov. 1995.

[5] T. Simlinger, H. Kosina, M. Rottinger, and S. Selberherr, "MINIMOS-NT: A generic simulator for complex semiconductor devices," in *ESSDERC'95 - 25th Europ. Solid-State Device Research Conf.*, H. de Graaff and H. van Kranenburg, Eds. Gif-sur-Yvette Cedex, France: Editions Frontieres, 1995, pp. 83–86.

[6] R. Vankemmel, W. Schoenmaker, R. Cartuyvels, and K. De Meyer, "Implementation of heterojunctions into the 2-D finite-element simulator PRISM: Some scaling considerations," *Solid-State Electron.*, vol. 35, no. 4, pp. 571–578, 1992.

[7] J. Tang and S. Laux, "MONTE: A program to simulate the heterojunction devices in two dimensions," *IEEE Trans. Computer-Aided Design*, vol. CAD-5, pp. 645–652, Apr. 1986.

[8] K. Yang, J. East, and G. Haddad, "Numerical modeling of abrupt heterojunctions using a thermionic-field emission boundary condition," *Solid-State Electron.*, vol. 36, no. 3, pp. 321–330, 1993.

[9] J. Jones, G. Tait, S. Jones, and D. Katzer, "DC and large-signal time-dependent electron transport in heterostructure devices: An investigation of the heterostructure barrier varactor," *IEEE Trans. Electron Devices*, vol. 42, pp. 1393–1403, Aug. 1995.

[10] D. Schröder, *Modeling of Interface Carrier Transport for Device Simulation*. Berlin: Springer, 1994.

[11] R. Bank and D. Rose, "Parameter selection for Newton-like methods applicable to nonlinear partial differential equations," *SIAM J. Numer. Anal.*, vol. 17, no. 6, pp. 806–822, 1980.

[12] ——, "Global approximate newton methods," *Numer. Math.*, vol. 37, pp. 279–295, 1981.

[13] H. van der Vorst, "BI-CGSTAB: A Fast and smoothly converging variant of BI-CG for the solution of nonsymmetric linear systems," *SIAM J. Sci. Stat. Comput.*, vol. 13, no. 2, pp. 631–644, 1992.

[14] C. Fischer and S. Selberherr, "Optimum scaling of non-symmetric jacobian matrices for threshold pivoting preconditioners," in *Int. Workshop on Numerical Modeling of Processes and Devices for Integrated Circuits NUPAD V*, Honolulu, HI, 1994, pp. 123–126.

[15] Y. Saad, "Preconditioning techniques for nonsymmetric and indefinite linear systems," *J. Comp. Appl. Math.*, vol. 24, pp. 89–105, 1988.

[16] P. Bhattacharya, Ed., *Properties of Lattice-Matched and Strained Indium Gallium Arsenide*. no. 8 in *EMIS Datareviews Series*, IEE INSPEC, 1993.

Thomas Simlinger was born in Mödling, Austria, on July 17, 1963. He received the degree of "Diplomingenieur" in communication engineering from Vienna University of Technology, Vienna, Austria, in 1992, and the Ph.D. degree from the same university in 1996.

Since 1996, he has been an Assistant Researcher at the Institute for Microelectronics, Vienna University of Technology.

Helmut Brech received the "Diplom" degree in electrical engineering from the University of Ulm, Germany, in 1995. His thesis was devoted to long wavelength lasers on GaAs. Currently, he is pursuing the Ph.D. degree at the Siemens Corporate Technology, Munich. His interests include development of models for physical device simulation, HEMT characterization, and optimization.

Thomas Grave was born in Frankfurt, Germany, in 1951. He received the diploma in physics and the Ph.D. degree from the University of Heidelberg, Germany, in 1975 and 1979, respectively.

From 1979 to 1983, he was an Assistant Researcher at the Institute of Applied Physics, the University of Heidelberg, working on optoelectronic and nonlinear optical effects in Ge and InSb. In 1983 and 1984, he was with the Max Planck Institute for Plasma Physics, Garching, Germany, where he participated in nuclear fusion research. Since 1984, he has been with the III–V electronics department of Siemens Corporate Technology, Munich, Germany, where he first was responsible for MESFET process development. This included the technology of a GaAs 1K SRAM and a SAGFET process applied to analog-to-digital converter IC's. For the last four years, he has been engaged in the development of GaAs-based pHEMT's for low noise, power, and millimeter wave applications.

Siegfried Selberherr (M'79–SM'84–F'93) was born in Klosterneuburg, Austria, on August 3, 1955. He received the degree of "Diplomingenieur" in control theory and industrial electronics from the Vienna University of Technology, Vienna, Austria, in 1978.

Since that time, he joined the "Institut für Allgemeine Elektrotechnik und Elektronik" (formally "Institut für Physikalische Elektronik") at the Vienna University of Technology. He finished his thesis on "Two Dimensional MOS-Transistor Modeling" in 1981. Since 1984, has been holding the "venia docendi" on "Computer-Aided Design" as Professor. He has been the head of the "Institut für Mikroelektronik" at the Vienna University of Technology since 1988. In 1994, he has been appointed head of the "Computing Services Center" of the Vienna Unversity of Technology. His current topics are modeling and simulation of problems for microelectronics engineering. He authored and co-authored more than 250 publications in journals and conference proceedings. He also authored *Analysis and Simulation of Semiconductor Devices* (Springer, 1984)

Dr. Selberherr received the "Dr. Ernst Fehrer" award in 1983, the award of the "Nachrichtentechnischen Gesellschaft" in 1985, was honored with the "Dr. Herta Firnberg Staats-preis" in 1986, and received the "Heinz Zemanek" award in 1987. In 1993, he was elected a Fellow of the IEEE for pioneering work in numerical analysis of semiconductor devices and their processes. In 1994, he was honored with the "Wilhelm Exner Medal." He has been a member of the Association for Computing Machinery since 1979, the Society of Industrial and Applied Mathematics since 1980, and the "Verband deutscher Elektrotechniker" since 1984. He has been the Editor of *The Transactions of the Society for Computer Simulation* since 1983, of *Mikroelektronik* since 1988, and of the Springer-Verlag book series, *Computational Microelectronics*, since 1985. He was also the Editor of *Electrosoft* from 1986 to 1991. Since 1994, he has been serving on the Programme Advisory Board of *Electron Technology*.